KAPITEL 9 / *CHAPTER 9*
SWITCHED RELUCTANCE MOTORS. DESIGN, SIMULATION, CONTROL
ВЕНТИЛЬНО-ІНДУКТОРНІ ДВИГУНИ. ПРОЕКТУВАННЯ, МОДЕЛЮВАННЯ, КЕРУВАННЯ. ВЕНТИЛЬНО-ИНДУКТОРНЫЕ ДВИГАТЕЛИ. ПРОЕКТИРОВАНИЕ, МОДЕЛИРОВАНИЕ, УПРАВЛЕНИЕ

DOI: 10.30890/2709-2313.2021-07-08-017

Introduction

Today, electric motors are considered as an integral part of household electrical appliances and power tools, electric vehicles of different capacity for various purposes, and the vast majority of industrial equipment, units and robots. Such a wide application causes the availability of a large variety of electric motor types, respectively focused on different tasks. Modern electric motors are distinguished by the type of power supply (DC and AC), design features, operation modes, control methods, etc.

Given the trends of the recent years, we can state that electric vehicles will become soon one of the largest areas of applying electric motors [1]. The gradual transition to electric traction has already been going on for the last few decades. However, the course in support of green technologies, which has taken by most of the developed world, promises a sharp reduction in producing internal combustion engine vehicles in the near future, and subsequent complete refusal of them in favor of electric vehicles.

The electric transport industry includes several different directions:

- powerful electric trains;
- urban public vehicles – buses, trolleybuses, trams;
- electric cars;
- low-power vehicles – electric scooters, electric bicycles, segways, unicycles, electric wheelchairs, etc.;
- light aircrafts – electric planes, quadcopters.

Depending on the desired parameters of electric vehicles, such as carrying capacity, maneuverability, traction and performance characteristics, the most appropriate types of electric motors that are able to provide these characteristics should be chosen.

Thus, until recently, brushed DC motors, connected directly to the DC power supply of 550-600 V, were mainly used as traction motors for urban public transport (trolleybuses, trams) with a capacity of hundreds of kilowatts [2]. Such motor type is featured by high starting torque, simple control and reversing, nearly linear control characteristics, high efficiency, and the ability to adjust the rotational speed in wide range. However, due to enhancement of power electronics and microprocessor technology in recent decades, brushed DC motors are being actively replaced by asynchronous AC motors [2]. Although the last ones require a more complex control system with DC to AC converting unit, they are cheaper and structurally simpler, have a simple start-up and high dynamic characteristics. In addition, they need less maintenance and have much higher reliability due to elimination of brush-collector

units.

Asynchronous electric motors are also used for traction in some models of electric cars with a capacity of tens of kilowatts [3]. However, such motors are not optimal in this application, because significant energy losses in the rotor bars and thus not high enough efficiency are inherent for them. This is crucial for electric cars supplied from autonomous battery, unlike trolleybuses and trams. Through this, most modern electric cars are equipped with brushless synchronous DC motors with permanent magnets, which are characterized by smooth speed control, low weight and dimensions [4]. Still, for all their advantages, permanent magnet motors have a quite complex multipole design and low specific torque, which determines the ordinary dynamic performance of the cars. Besides, permanent magnet motors have high cost given by use of rare earth metals (neodymium-based alloys) as magnets [4]. To improve the dynamic performance, electric cars with permanent magnet motors may be additionally equipped with asynchronous motors.

DC motors on permanent magnets are also mainly used in low-power electric bicycles, scooters, unicycles, etc. [4]. The most critical parameters of such vehicles are mass and dimensions, and the motor efficiency as well, while their speed is mostly limited to 25 - 50 km/h.

It is also known about the use of synchronous motors on electromagnets in electric cars [5]. Such motors, unlike asynchronous ones, are not able to self-starting, so to ensure high starting characteristics they are equipped with additional structural elements that provide fast asynchronous starting. However, synchronous motors on electromagnets have a lower cost compared to motors on rare earth permanent magnets, also they have higher power and speed stability, as well as the best ability to recuperating energy during braking, thus saving battery power.

Recently, a switched reluctance motor (SRM) is considered as promising motor type for use in electric vehicles. SRMs have simple and technological design, high reliability and maintainability, a wide range of speed control and high efficiency. Besides, these motors are produced using electrical steel or ferromagnetic materials, so they are much cheaper than the ones on permanent magnets [2, 6]. Due to their advantages, SRMs are regarded as an alternative to permanent magnet motors. However, their widespread use in electrical vehicles is restrained by such their drawbacks as low specific torque and its significant ripple. The last ones can be eliminated by forming a special current shape in the stator windings and by improving the motor topology through optimizing the shape and number of the stator and rotor poles.

It should be noted that the continuous progress in power and information electronics, improvement and invention of new structural and electrical materials lead to creation of novel approaches to designing the electric drive systems for vehicles. Thus, recently there has been a trend towards using combined solutions in this area. It is known, for instance, about successful combination of construction principles of an internal permanent magnet motor and a synchronous reluctance motor, which gives significant advantages in most basic parameters [7]. In addition, the change of the element base characteristics and the steady development of technologies and design ideas lead to the fact that the known earlier but limited in use solutions are becoming

in demand. In particular, this concerns to the switched reluctance motor type. The interest in SRMs has increased recently in the context of a significant increase in the cost of neodymium permanent magnets, which are widely applied today in electric motors of vehicles [6].

This chapter is devoted to switched reluctance motors. In view of the foregoing, it is obvious that the improvement of SRM characteristics is an urgent task for the development of the electric transport industry. The following subsections of the chapter will consider the principles of construction and operation of classical SRMs, the ways to improve their design, to maximize the torque and to minimize its ripples, as well as to increase the energy efficiency.

To carry out the research presented in this chapter, modern software for mathematical simulation was used.

9.1. Typical operation and design principles of switched reluctance motors

The switched reluctance motor is classified as a brushless DC electric motor also known as an electronically commutated motor or synchronous DC motor. This motor type runs by reluctance torque. Currently, many different topologies of switched reluctance motors are known [6, 8]. Fig. 1 gives two common SRM designs: with an inner rotor (a) and with an outer rotor (b).

The design of SRM shown in Fig. 1 (a) can be called a classic one. It is very simple: the toothed cylindrical rotor is located inside the toothed stator with concentrated phase windings installed on teeth-poles [6]. The opposite windings of the same phase can be electrically connected in series or in parallel, and they can have cumulative or differential magnetic coupling. Rotor and stator are made up from magnetically soft materials (electrical steel or ferromagnets) with high magnetic permeability and low hysteresis losses. In order to reduce eddy current losses, both the rotor and the stator are produced not solid, but laminated.

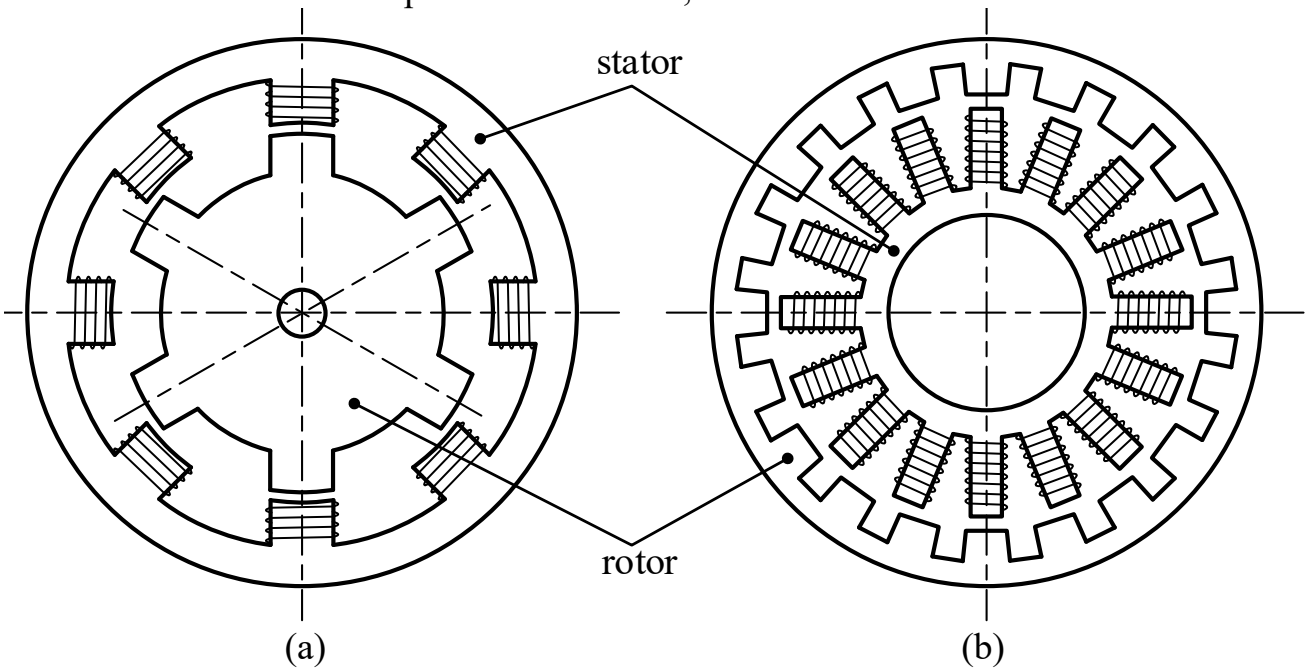

Figure 1 – Switched reluctance motor designs

The operation principle of switched reluctance motor is as follows. Unipolar current pulses energize the stator pole windings in the phase sequence order, which creates a magnetic flux closing through the rotor between two windings of the active phase. The number of the rotor poles m is not equal to the number of the stator poles k, usually $k > m$. The most commonly used ratios m / k are: 4/6, 6/8, 8/12 [6, 9]. The poles are placed in a way that there is always a shift between the poles of the rotor and the stator. So that, when the current pulses are applied to the windings of the active phase, the rotor begins turning, trying to reach a position providing a low reluctance path for the magnetic flux. The torque that develops under such conditions is called reactive.

Fig. 2 shows as an example the formation of magnetic flux and resulting rotation of the rotor for three-phase SRM topology with the ratio $m / k = 4/6$ [9].

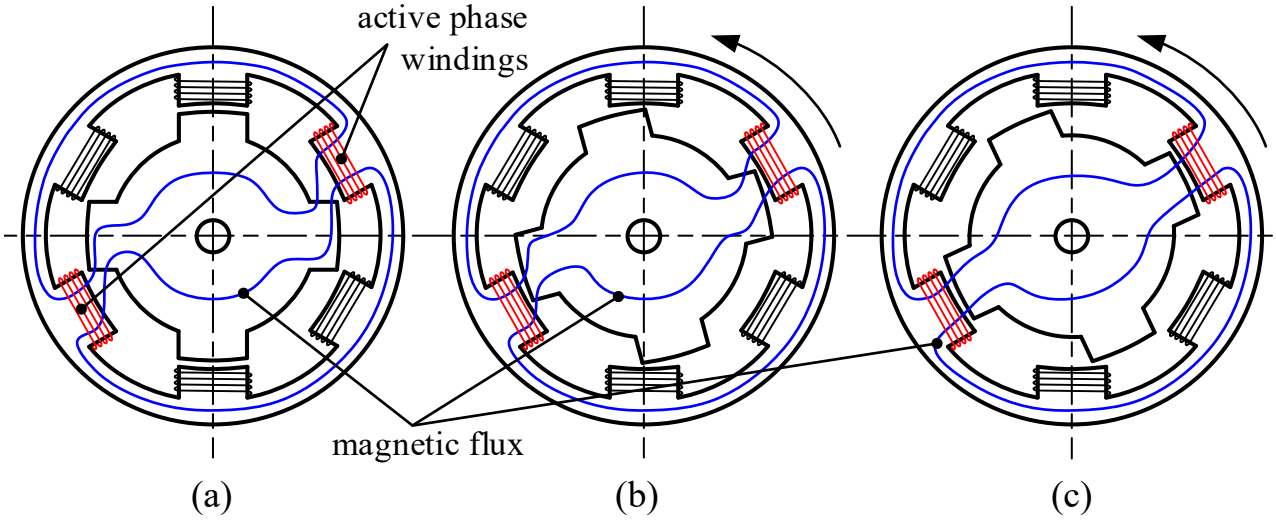

Figure 2 - Rotation of SRM rotor

As can be seen from Fig. 2, in the order from (a) to (c), after applying control pulses to windings of one of the three phases, the rotor starts rotating, which leads to shortening the magnetic field lines. When the active poles of the stator and the rotor reach complete axial alignment, the reluctance to magnetic flux becomes minimal, but the torque at this point is equal to zero, so the control pulses energize the next phase windings to continue the rotation, and then the process is repeated.

The rotor speed is regulated by the frequency of current pulses on the stator pole windings. A frequency inverter is used for this purpose. The order of pulses on the phase windings is determined considering the actual position of the rotor, which is monitored using a special sensor – encoder.

Fig. 3 gives two common ways of forming control pulse sequences for phases 1, 2 and 3 of three-phase SRM (Fig. 2).

The case in Fig. 3 (a) is the simplest: the control pulse for every next phase starts immediately after finishing the control pulse for the previous one, and the duty cycle is equal to 1/3. In the other case (Fig. 3 (b)), two of the three phases operate simultaneously during certain time intervals, and the duty cycle is equal to 1/2. This makes it possible to increase the total number of the rotor positions by the number of

intermediate ones due to the joint operation of the two phases during some intervals, thereby reducing torque ripples and resulting in smoother rotor movement. Both cases shown in Fig. 3 are reversible, i.e. the reverse order of control pulses for the phases causes the rotor rotation in the other direction.

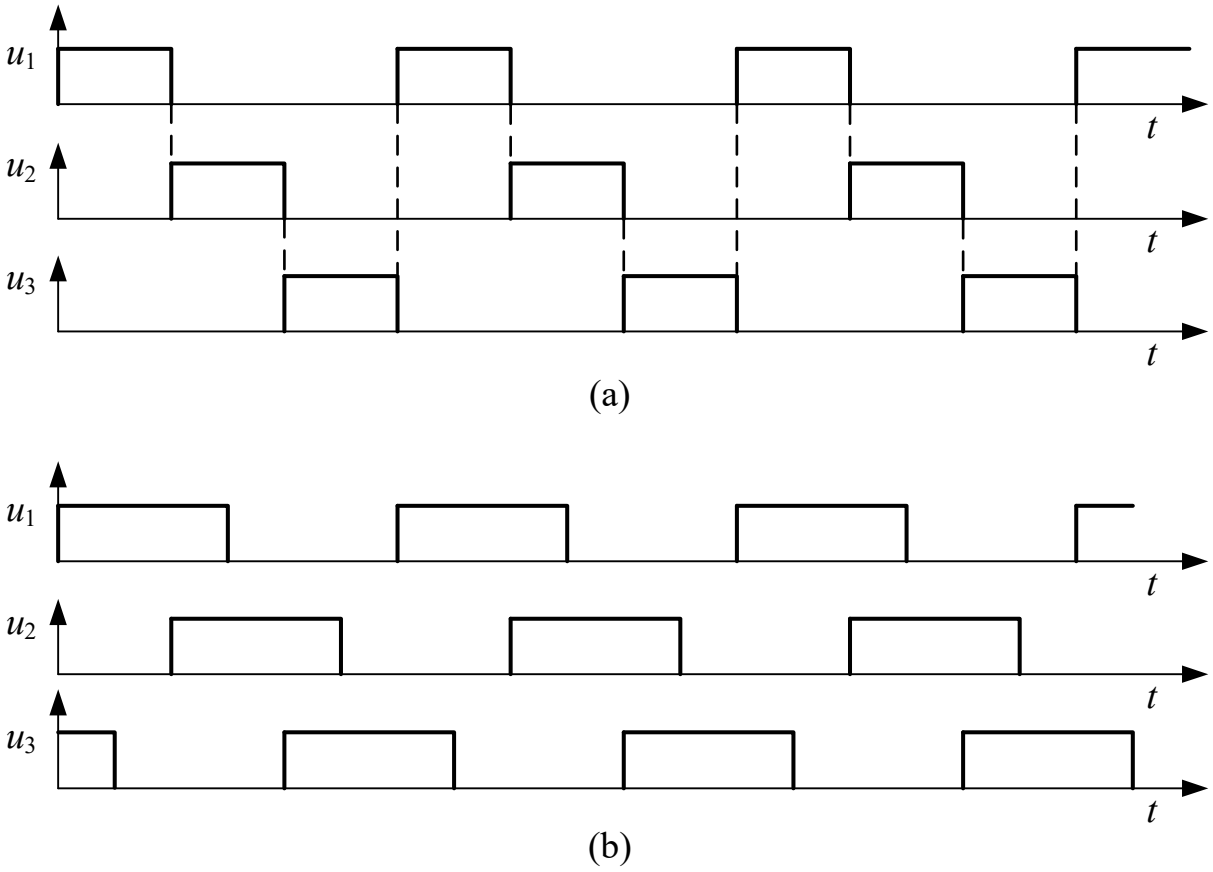

Figure 3 - The ways of forming control pulse sequences for three-phase SRM

In general, the torque ripple magnitude in switched reluctance motors of classical topology depends on the pole number and control algorithm: the larger pole number and the more "intelligent" control algorithm, the higher rotation smoothness can be achieved. However, it is obvious that the reduction of torque ripples in this way is accompanied by a significant complication of the motor topology and its control system. Another disadvantage of the classical topology of SRMs is a solid rotor design, which involves significant material costs and low torque.

It is possible to get rid of SRM classical topology drawbacks in the following ways: choice of the optimal shape of the poles and their ratio, improve of the rotor design, development of an effective control algorithm, and use of a special form of the stator winding current.

In the next subsections, SRM motor with an improved topology will be represented, its operation features will be investigated and the efficiency of the proposed solutions will be evaluated.

9.2. Operation features and pole ratios of U-shaped pole switched reluctance motors

In [10], a new topology of the SRM is proposed (Fig. 4 (a)). As can be seen from the figure, the poles of the stator and rotor are U-shaped. Their number is variable. The optimal pole number and stator/rotor pole ratio can be calculated based on specific given conditions, as will be shown below. The stator and the rotor of this SRM are not solid: the soft magnetic poles are incorporated into the non-magnetic, ceramic or plastic, retaining structure, which reduces the magnetic material consumption and the total weight of the motor. Besides, in contrast to the classical topology of SRM, shown in Fig. 1 and Fig. 2, the stator and rotor poles in the proposed topology have a modular structure and can be produced separately by cheaper technology.

The stator poles are activated individually in their turn, not in pairs as provided by the classical topology of SRMs. In this case, depending on the desired SRM characteristics, it is possible to use various algorithms to form control pulse sequences for the stator pole windings.

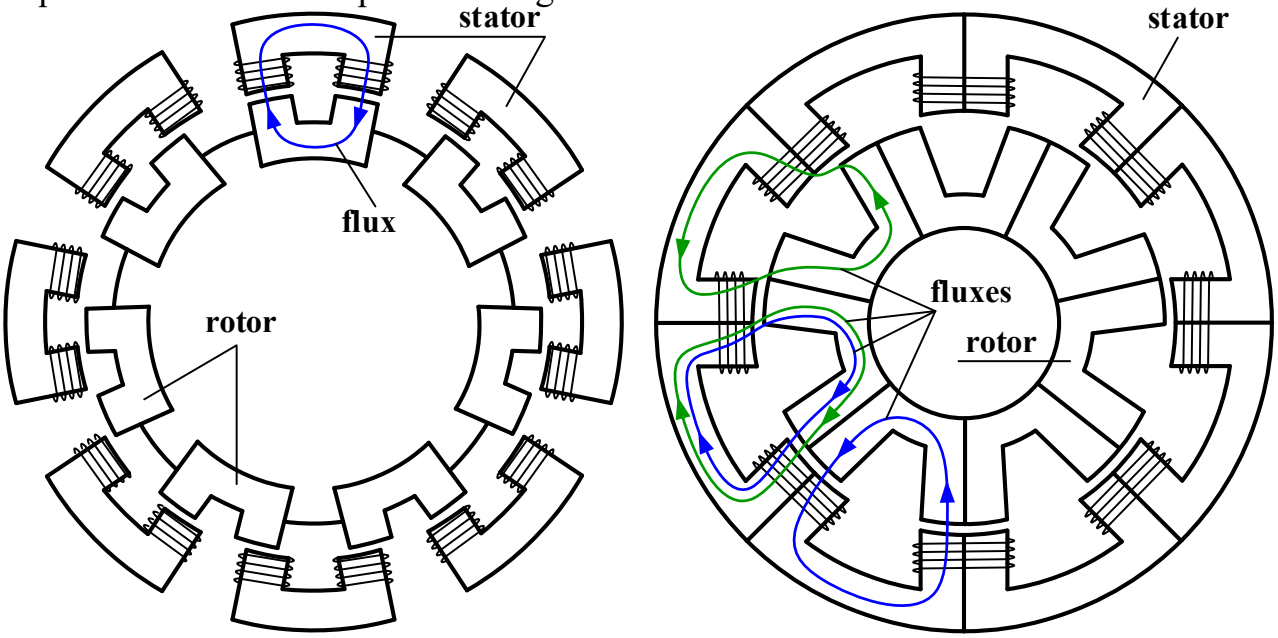

Figure 4 – SRM topologies with U-shaped poles

It should be pointed that the SRM topology with U-shaped poles requires additional space to place the windings at the stator poles (see Fig. 4 (a)), which can be obtained by reducing the rotor radius or by decreasing the density of the stator poles, that however leads to motor specific torque decrease. To prevent the reduction of the specific torque, it is proposed to use paired windings for the stator poles (Fig. 4 (b)), so that the windings are wound on the teeth of two adjacent poles together, which makes it possible to accurately place them in the pole windows without using additional space and thus provides the higher density of the poles. At the same time, the paired windings create magnetic fluxes in both poles at once, which should be considered when developing the control algorithm for the poles. Also, it is necessary

to note that the paired U-shaped poles are magnetically isolated from each other, so the distribution of magnetic fluxes between them differs from the one in SRM with the classical topology.

It is important to take into account that when the stator pole is activated, the magnetic flux passes not only through the working one, but also through the near poles of the rotor. This reduces the force of the rotor working pole attraction to the stator.

Theoretically, the magnetic flux generated by the stator active pole winding is distributed between all the rotor poles at the same time, but in practice, it is sufficient to consider the effect of magnetic flux only on two adjacent rotor poles (Fig. 5), because the effect on the other poles is too weak and can be neglected. Let's consider the processes of magnetic flux distribution between the rotor poles and its stray using Fig. 5.

Assume that the magnetic flux Φ_Σ is created by the active stator pole **1-s**. It is divided into three main components: the flux Φ_1 passing through the rotor pole **1-r**, the flux Φ_2 passing through the adjacent rotor pole **2-r**, and the stray flux Φ_3, which does not perform any useful work and is closed through the working pole of the stator **1-s** and the air gap between its teeth. Therefore:

$$\Phi_\Sigma = \Phi_1 + \Phi_2 + \Phi_3. \quad (1)$$

Let the rotor moves clockwise, then the pole **1-r** pulls the rotor in the forward direction, while the pole **2-r** pulls it in the opposite one, thus braking it. The stator pole, which is adjacent to the working one, is denoted in Fig. 5 as **2-s**. The distance between the nearest stator poles is denoted as l and the distance between the poles of the stator and the rotor as x.

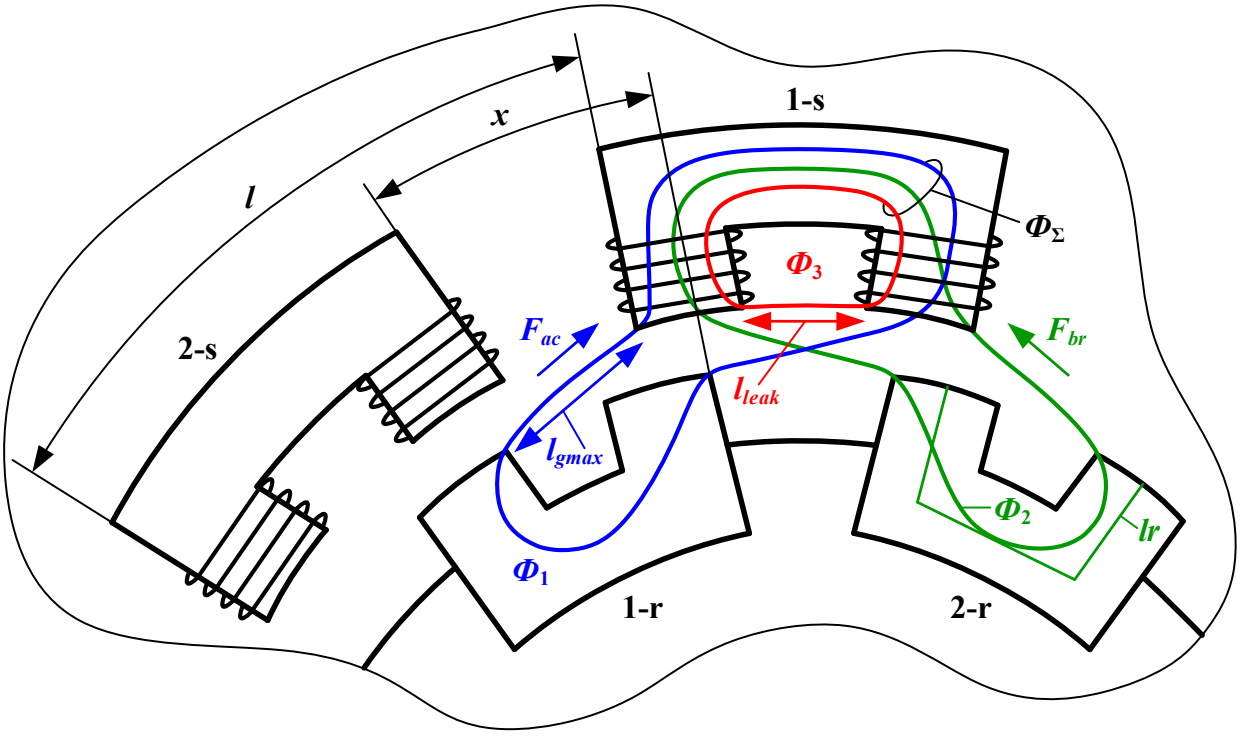

Figure 5 – Magnetic flux distribution between two adjacent rotor poles

To evaluate the effect of each of the three components of the total magnetic flux, let's obtain the corresponding mathematical relationships.

First, let's express the magnetic field strength H through the magnetic flux Φ:

$$\left.\begin{array}{l} H = \dfrac{B}{\mu_0 \mu} \\ \Phi = BS \end{array}\right\} \Rightarrow H = \frac{\Phi}{S \mu_0 \mu}, \tag{2}$$

here B is magnetic flux density, μ_0 is the permeability of free space, μ is relative permeability of the material, S is the surface area through which the magnetic flux passes.

Next, let's compose the equations for three magnetic circuits according to Kirchhoff's second law:

$$\begin{aligned} I \cdot N &= \frac{\Phi_\Sigma l_s}{S_g \mu_0 \mu_m} + \frac{\Phi_1 l_r}{S_g \mu_0 \mu_m} + \frac{\Phi_1 l_{g\max}}{S_g \mu_0 \mu_g}(1 - x^*) \\ I \cdot N &= \frac{\Phi_\Sigma l_s}{S_g \mu_0 \mu_m} + \frac{\Phi_2 l_r}{S_g \mu_0 \mu_m} + \frac{\Phi_2 l_{g\max}}{S_g \mu_0 \mu_g} x^* \\ I \cdot N &= \frac{\Phi_\Sigma l_s}{S_g \mu_0 \mu_m} + \frac{\Phi_3 l_{leak}}{S_g \mu_0 \mu_g}, \end{aligned} \tag{3}$$

here I is the stator winding current, N is the number of stator winding turns, l_s, l_r are the lengths of the magnetic circuit of the stator and the rotor respectively, S_g is the air gap area, μ_m, μ_g are the relative magnetic permeability of the magnetic circuit and the air gap respectively, $\mu_g \approx 1$, l_{leak}, l_{gmax} are the air gap between the stator pole teeth and the maximum stator and rotor poles' gap respectively, x^* is the distance between the poles of the stator and the rotor, normalized relative to 1, $x^* = x/l$, x is the distance between the poles of the stator and the rotor.

Subtracting the second equation from the first one in (3), and then subtracting the third equation from the first one, we obtain the ratio between the magnetic fluxes:

$$\begin{aligned} &\frac{\Phi_2}{\Phi_1} = \frac{l_r + l_{g\max}(1 - x^*)\mu_m}{l_r + l_{g\max} x^* \mu_m}; \frac{\Phi_3}{\Phi_1} = \frac{l_r + l_{g\max}(1 - x^*)\mu_m}{l_{leak}\mu_m}; \\ &\frac{\Phi_3}{\Phi_2} = \frac{l_r + l_{g\max} x^* \mu_m}{l_{leak}\mu_m}; \end{aligned} \tag{4}$$

Adding two first equations, then adding and subtracting Φ_1, and considering (1), we obtain the ratio for Φ_1. In the same way, we obtain the ratios for the fluxes Φ_2, Φ_3:

$$\Phi_1 = \frac{\Phi_\Sigma}{1 + \frac{q_1 + 1 - x^*}{q_1 + x^*} + \frac{q_1 + 1 - x^*}{q_2}},$$

$$\Phi_2 = \frac{\Phi_\Sigma}{1 + \frac{q_1 + x^*}{q_1 + 1 - x^*} + \frac{q_1 + x^*}{q_2}},$$

$$\Phi_3 = \frac{\Phi_\Sigma}{1 + \frac{q_2}{q_1 + x^*} + \frac{q_2}{q_1 + 1 - x^*}}, \quad (5)$$

here q_1, q_2 are the parameters, which depend on geometry and material of the poles:

$$q_1 = \frac{l_r}{\mu_m l_{g\max}}; \quad q_2 = \frac{l_{leak}}{l_{g\max}}, \quad (6)$$

Provided that the components of the forces are directed horizontally, magnetic flux Φ_1 makes the force F_{ac_x}, which accelerates the rotor pole, whereas the flux Φ_2 brakes it with the force F_{br_x}. Thus, the total force F_Σ is the difference between accelerating and braking forces:

$$F_\Sigma = F_{ac\_x} - F_{br\_x}, \quad (7)$$

The total torque M_Σ developed by the motor is calculated as a product of the total force and a radius R of the rotor:

$$M_\Sigma = F_\Sigma \cdot R. \quad (8)$$

The total current I_Σ of the stator pole winding can be calculated as follows:

$$I_\Sigma = I_{ac} + I_{br} + I_{leak}, \quad (9)$$

here I_{ac}, I_{br} are the currents inducing the accelerating force F_{ac_x} and the braking force F_{br_x} respectively, I_{leak} is the current inducing the stray flux.

The forces F_{ac_x} and F_{br_x} are the functions of the distance between the stator pole and a corresponding rotor pole, and can be expressed in terms of the generalized force F:

$$F_{ac\_x} = F(1 - x^*); F_{br\_x} = F(x^*). \quad (10)$$

The generalized force F is calculated as follows:

$$F(x^*) = \frac{1}{2\mu_0 S_g} \cdot \left(\frac{I(x^*)L(x^*)}{N} \right)^2 = k\left(I(x^*)L(x^*) \right)^2, \tag{11}$$

here $L(x^*)$ is the generalized inductance, which is associated with one of the fluxes, k is the coefficient, which depends on the pole parameters.

The generalized inductance is calculated by the formula:

$$L(x^*) = \frac{N^2 \mu_0 S_g \mu_m}{l_m + l_{g\max} x^* \mu_m} = \frac{\frac{N^2 \mu_0 S_3 \mu_m}{l_{g\max} \mu_m}}{(l_m / (\mu_m l_{g\max}) + x^*)} = \frac{c_1}{c_2 + x^*}, \tag{12}$$

According to the total force expression, we can plot the stator pole attraction force (total force) versus rotor pole normalized distance x^* (Fig. 6).

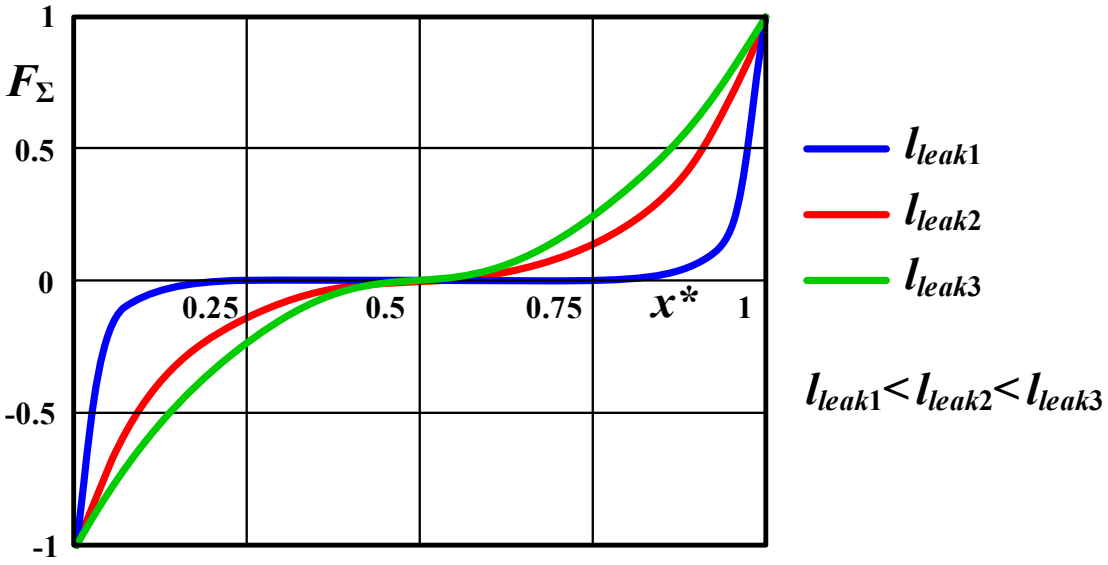

Figure 6 – The total force over the normalized distance x^* plot

We can distinguish three different intervals on the plot.

$x^* > 0{,}5$:

In this interval, the rotor pole conducting magnetic flux Φ_1 is closer to the active stator pole than the pole conducting the flux Φ_2. This provides a positive total force in the direction of the rotor movement, $F_\Sigma > 0$.

$x^* < 0{,}5$:

In this interval, the rotor pole conducting magnetic flux Φ_1 is further from the active stator pole than the pole conducting the flux Φ_2. This provides a negative total force in the direction of the rotor movement, $F_\Sigma < 0$.

$x^* = 0{,}5$:

In this point, the magnetic fluxes through the both rotor poles are equal, $\Phi_1=\Phi_2$, whereas the stray flux Φ_3 is maximal. So that, the total force is zero, $F_\Sigma = 0$.

It is also important to pay attention to the dependence of the total force on the distance l_{leak} between the teeth of the stator pole. Thus, the smaller distance the smaller value of the total force we have, which is logical considering the increase of the stray flux Φ_3. Therefore, the condition $l_{leak} >> l_g$ should be kept during the entire operating time to provide efficient motor operation.

Obviously, another important condition for ensuring high efficiency of SRM operation, as well as minimal torque pulsations under minimal total current of the stator pole winding is the tendency of the braking force F_{br} to zero. This requires the working rotor pole to be as close as possible to corresponding stator pole when activating it during rotor rotation. Thus, the topology of the SRM, namely the number of stator and rotor poles and their ratio, plays a crucial role.

To evaluate the efficiency of the SRM, let's use the ratio k_F of braking and accelerating forces affecting the working rotor pole:

$$k_F=1 - F_{br\_x} / F_{ac\_x}. \quad (13)$$

The values of k_F can vary in the range [0; 1] for $x^* \geq 0.5$, where the zero value corresponds to complete inefficiency and the value 1 corresponds to the maximum efficiency.

It is important to note that the possibility of creating torque is provided when the number of stator poles k exceeds the number of rotor poles m, $k > m$. The maximum efficiency of SRM, $k_F = 1$, is achieved by increasing k and m to infinity, which is practically unattainable. Therefore, it is advisable to maximize the efficiency of the motor at a fixed number of stator and rotor poles.

Let's consider and analyze several possible topologies of SRM. The topologies with stator/rotor poles combinations $(n+1)/n$, $(2n+1)/n$, $(2n+2)/n$ for $n = 4$ are shown in Fig. 7 (a), (b), (c) respectively.

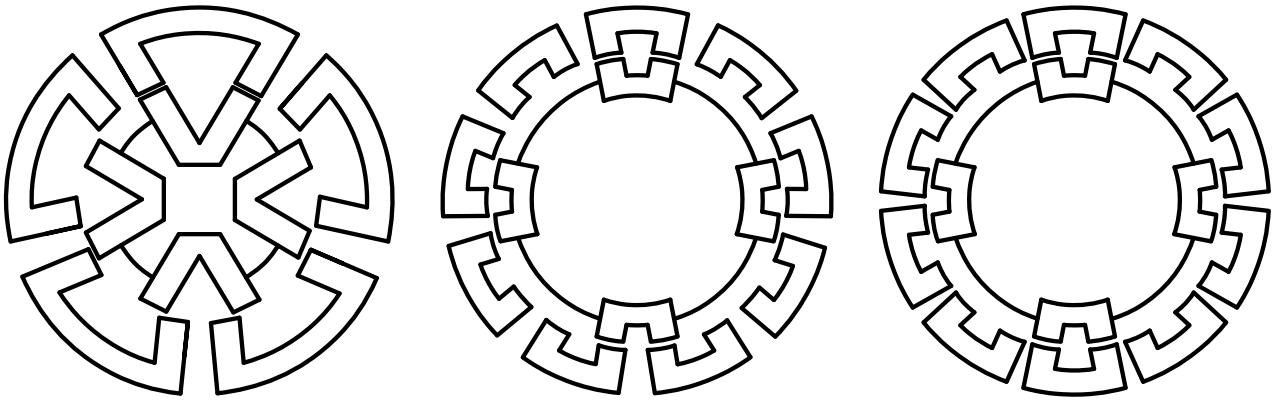

(a) (b) (c)

Figure 7 – SRM topologies: (a) $(n+1)/n$, (b) $(2n+1)/n$, (c) $(2n+2)/n$

As we can see from Fig. 7, in the topologies (b) and (c) the number of the stator

poles is significantly higher than the number of the rotor poles. This determines remote location of adjacent rotor poles relative to the active pair of rotor and stator poles, and obviously provides less braking force than the one in the topology (a). However, the topology (a) has a higher density of the rotor poles' location relative to the stator ones, which makes it possible to obtain a higher accelerating force, so, this topology is more preferable in practice.

It should be noted that the dimensional parameters of the stator and rotor poles should be chosen to provide the same cross sections of their teeth and the same distances between the teeth, because the magnetic fluxes passing through them are equal, so they have the same saturation conditions. The shape of the rotor poles is not so important and can be chosen based on the configuration of the SRM internal space. For example, in Fig. 7 (a) the shape of the rotor poles is triangular.

As mentioned earlier, it is possible to apply different control algorithms to SRM poles by activating one or more stator poles simultaneously or in certain sequences. Based on the fact that only one rotor pole can be located maximally close to the working stator pole at each time, it is obvious that the highest efficiency can be achieved if you activate exactly one rotor pole at each time point. When controlling several poles at the same time, it is possible to develop more force, but in this case the poles switch at the moments of less efficiency.

Fig. 8 shows the dependence of the force ratio k_F on the number of poles for the SRM topology $(n+1)/n$ with two control options: (a) one pole activation, (b) simultaneous activation of $[n/2]$ poles, where the result is rounded off to the nearest integer number. As can be seen from the figure, for the option of one pole activation, the increase of the number n causes significant increase of the ratio k_F, and at $n = 10$ k_F approximates 1. When simultaneously activating $[n/2]$ poles, the ratio k_F decreases if the number of poles increases due to shortening the distance difference between the accelerating and braking poles. It should be noted that in the last case, the even value of n provides higher efficiency because more stator poles can operate simultaneously.

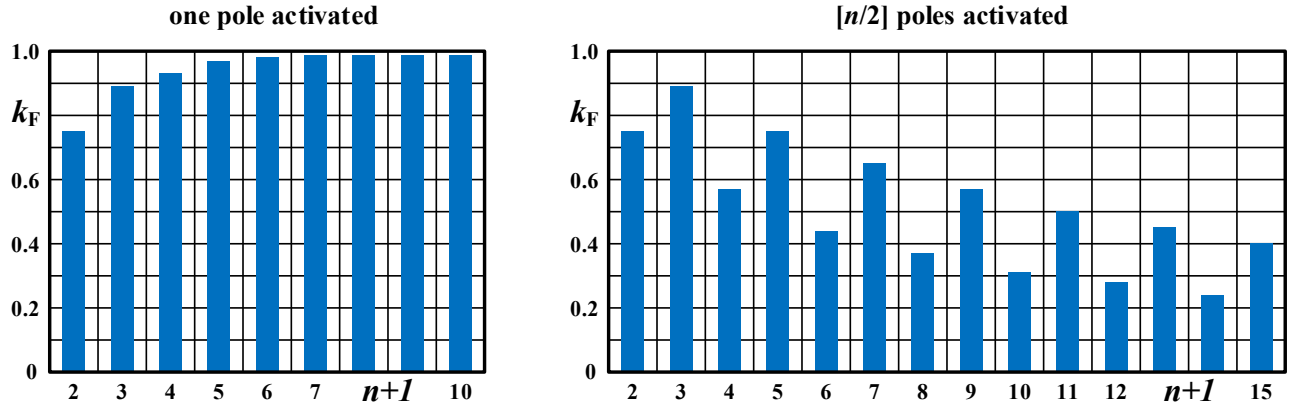

Figure 8 – Dependence of SRM force ratio k_F on the number of poles:
(a) one pole activation, (b) simultaneous activation of [n / 2] poles

The total force relation on n values for the defined motor dimensions (length l = 860 mm, diameter D = 520 mm) for one pole operation and $[n/2]$ pole operation

were evaluated and presented in Fig. 9 (a) and (b) respectively.

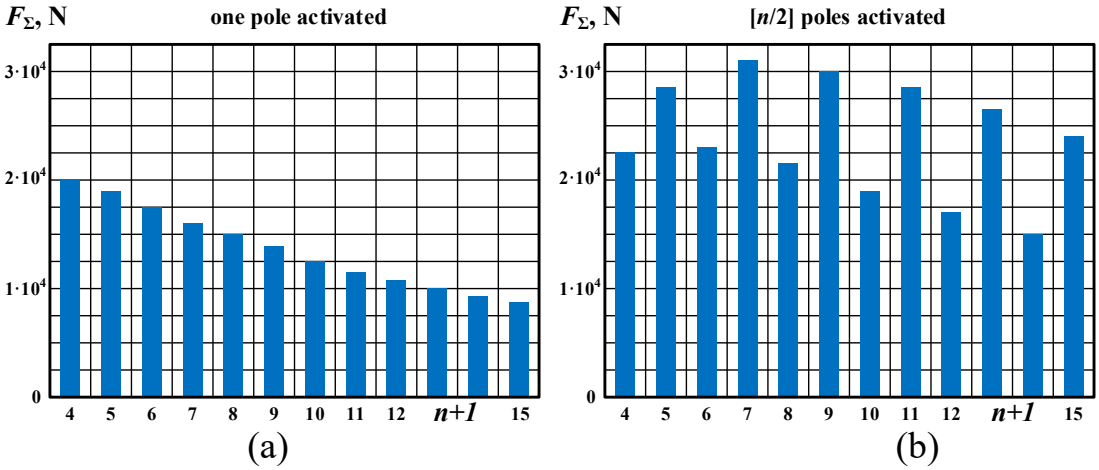

Figure 9 – Dependence of SRM total force on the number of poles:
(a) one pole activation, (b) simultaneous activation of [n/2] poles

As can be seen from the figure, if one pole activation is used, the maximum value of the force decreases with increasing the number of the poles. It can be explained by increasing the stray flux due to decreasing the pole dimensions. When using [n/2] poles, the maximum force is achieved at some value of n (here at n = 7), that should be taken into account in designing the motor.

In order to verify the theoretical positions, a motor with U-shaped poles located by (n+1)/n topology at n = 7 (when maximum force achieved F_Σ) and with the simultaneous control of three poles was developed and calculated. The SRM was placed in the standard motor case with the following dimensions: length l = 860 mm, diameter D = 520 mm. As a material for magnetic circuit, alsifer was chosen due to its high magnetic saturation and good frequency characteristics. The volume of the motor was reduced by 2.75 times and the power was increased by 6 times. Thus, the developed motor with the dimensions l = 313 mm, D = 520 mm provides a torque 1150 N/m and has a maximum speed 9375 rpm. The losses on the magnetic circuit magnetization reversal at the maximum operating frequency amounted to 8%.

In general, SRM with the proposed topology provides the same values of torque and its pulsation, as classical SRM. To improve these characteristics, it is advisable to analyze the pole shape and to choose the optimal one, as well as to apply the specific regulation of the current in the stator windings. So, further, let's consider certain ways to increase the torque and to decrease its pulsation.

9.3. Optimal pole profile of U-shaped pole switched reluctance motors

As mentioned earlier, the relatively low specific torque, as well as its significant ripple are the main disadvantages of SRM, caused by regular changes in the position of stator and rotor poles and, accordingly, by constant change in torque. Let's analyze the factors affecting these parameters.

To simplify the analysis, let's consider a model of a system consisting of three U-shaped poles – two rotor poles, **1-r** and **2-r**, and one stator pole **1-s** with a winding

1-w (Fig. 10).

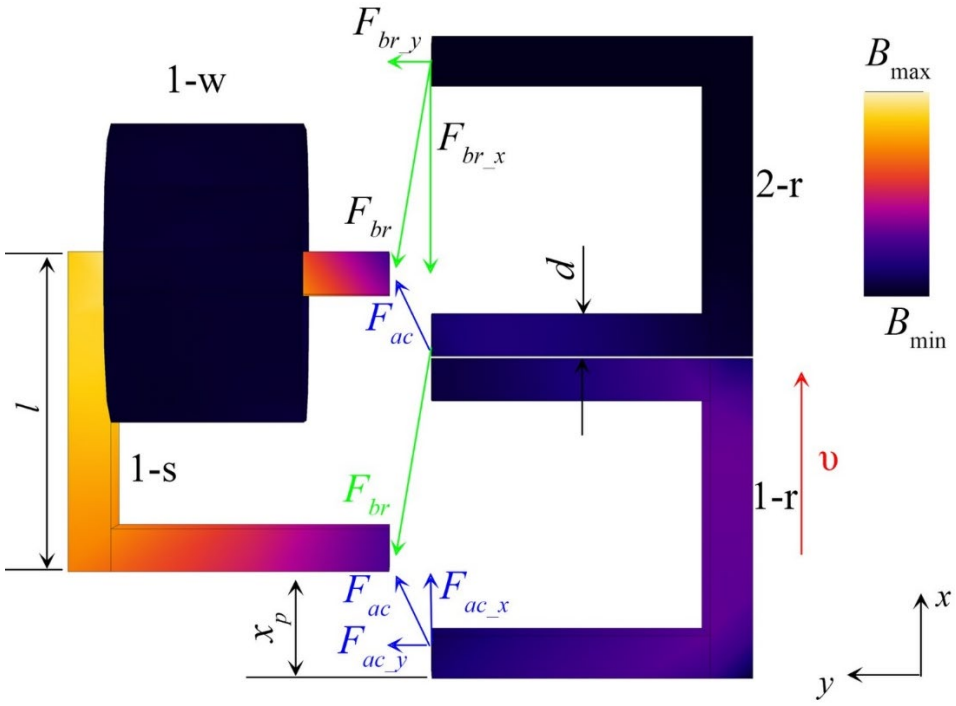

Figure 10 – The system of three U-shaped poles

The color gradient in Fig. 10 shows the change in the induction value B in the poles. As can be seen from the figure, a magnetic flux is induced in the stator pole, and is distributed between the two rotor poles. The magnetic flux closing through the rotor pole **1-r** produces a force F_{ac}, a component of which F_{ac_x} creates a torque, whose vector is co-directed with the velocity υ vector. In the same time, the magnetic flux closing through the pole **2-r** creates an oppositely directed braking force F_{br_x}. However, given the relative position of the poles, the force F_{ac_x} is bigger than the force F_{br_x}, the values of which are inversely proportional to the distance between the poles, so the rotor rotates in the positive direction. The force components F_{ac_y} and F_{br_y} attract the stator and rotor poles to each other and do not perform useful work.

Theoretically possible force F_Σ, which is determined by the magnetic induction B and the cross-sectional area of the pole S_g [11]:

$$F_\Sigma = \frac{S_g B^2}{2\mu_0}, \tag{14}$$

It is convenient to introduce the factor of electromagnetic energy use of SRM k_f^*:

$$k_f^* = \frac{F_{\Sigma x}}{F_\Sigma} = \frac{F_{ac} - F_{br}}{F}. \tag{15}$$

It becomes obvious from (15) that the factor k_f^* is low, which explains the low specific torque of SRM. It should be noted that the real value of the factor k_f^* is even lower, because the following phenomena are not taken into account in (15): stray flux formed in the stator pole, saturation of the magnetic circuit and the energy loss in the pole winding. In addition, the factor k_f^* depends on the relative position of the poles, which is determined by the parameter x_p, $k_f^* = f(x_p)$, so at a constant current of the stator pole windings for certain values of x_p the factor of electromagnetic energy use is critically low, which causes significant pulsation of the motor torque.

One of the ways to increase the torque and reduce the ripple is to optimize the shape of the poles, which is proposed in a number of studies [12, 13]. An alternative to this is the formation of stator winding current by a special law [14]. Next, the implementation of these two approaches is investigated.

When using the poles with a rectangular profile, there is a significant uneven distribution of the magnetic flux as well as the torque decrease caused by high concentration of the magnetic field at the pole edges (Fig. 11) producing the pole material saturation in these places, and consequently a decrease in the torque and the factor of electromagnetic energy use k_f^*. Additionally, the factor k_f^* decreases if the distance between the poles x_p (Fig. 10) does not exceed the width of the pole tooth d, because in this case the force component F_x acting along the x-axis and performing the useful work, is much smaller than the force component F_y ($F_x << F_y$).

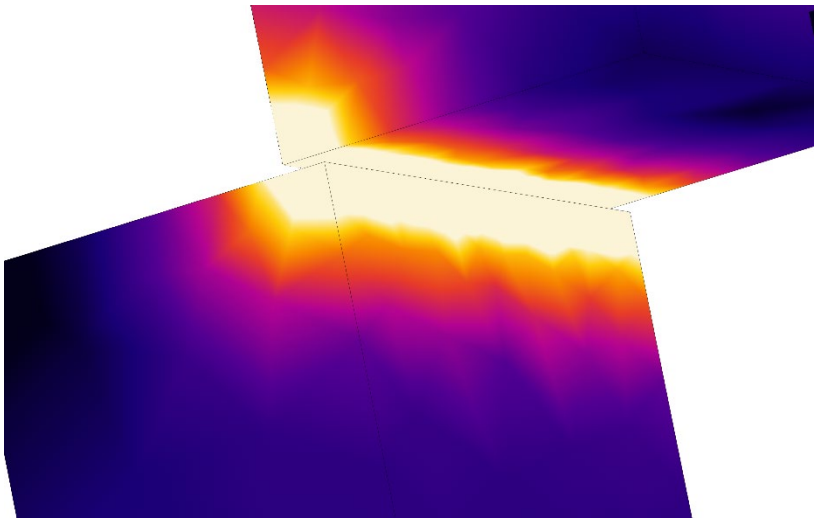

Figure 11 – The field concentrated at the edges of the poles with a rectangular profile

To eliminate this disadvantage in SRMs of classical topology, a more complex pole shape, often trapezoidal one with an extended profile (Fig. 12 (a)), is proposed to use in a number of studies. Such a pole shape really provides to develop a significant torque in a larger part of the rotation sector due to increasing the inductance of the system "stator pole - rotor pole". However, it has the following disadvantages: reduce of the factor of electromagnetic energy use k_f^* at the intersections of the poles caused by a significant increase in the force component F_y comparing to the component F_x ($F_x << F_y$), as well as the pole material saturation at the edges (Fig. 11).

For the proposed SRM structure consisting of U-shaped poles, this approach has the additional disadvantage. A substantial increase in the stray flux of the stator field caused by a significant reduction in the distance between the pole teeth at their expansion places makes it impossible to use this pole shape, in fact. Therefore, it is also advisable to analyze the trapezoidal pole with a narrowed profile, shown in Fig. 12 (b).

The pole faces should be formed at an angle of 45° with a length equaling to a half the pole width $d/2$. Then the induction density on the pole face will be almost even, because of the equidistance of the faces of the two poles. However, it should be noted that when using a trapezoidal pole with a narrowed profile, the effective gap width increases.

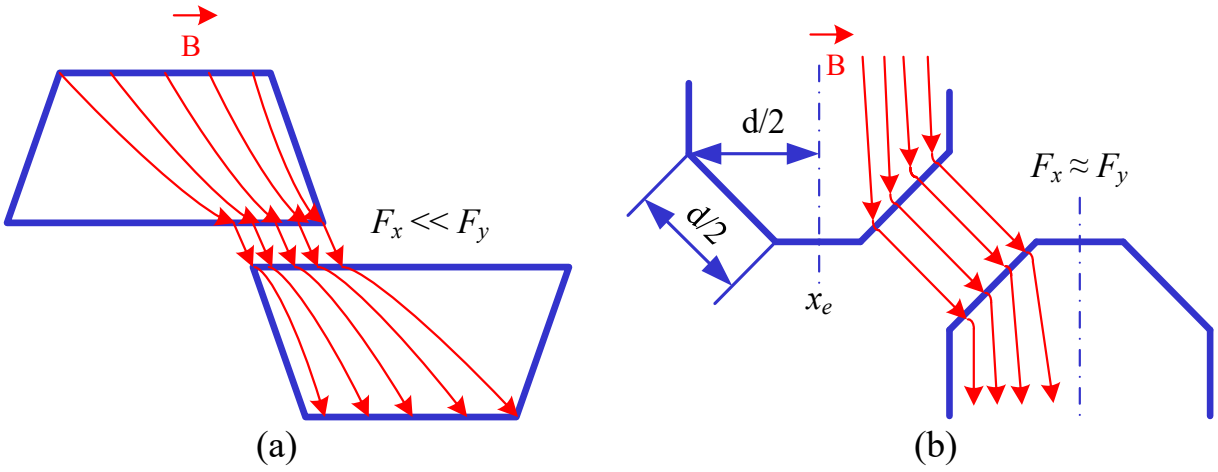

Figure 12 – Pole profiles: ***(a) trapezoidal pole with an extended profile, (b) trapezoidal pole with a narrowed profile***

Therefore, we can see, that the choice of the pole shape, providing the highest value of the factor k_f^* and torque, as well as minimal ripple, is a complicated task. So, it is convenient to use a mathematical model of SRM stator and rotor poles to evaluate the electromagnetic processes. The software environment of Comsol Multiphysics is considered as the most suitable for creating and studying such a model. In particular, the simulation software is used to analyze the induction distribution in the magnetic core and the rotational force formation.

The total force F_Σ that can be formed in the stator pole is calculated by the formula (14). Since the induction B in the core is a function of three spatial coordinates, $B = f(x, y, z)$, the formula (14) will be transformed as follows:

$$F = \frac{\iint_S B(x, y, z_0)^2 \, dxdy}{2\mu_0}, \tag{16}$$

here S is a level surface at $z = z_0$ intersecting the stator pole in the plane of the highest induction density, as shown in Fig. 13.

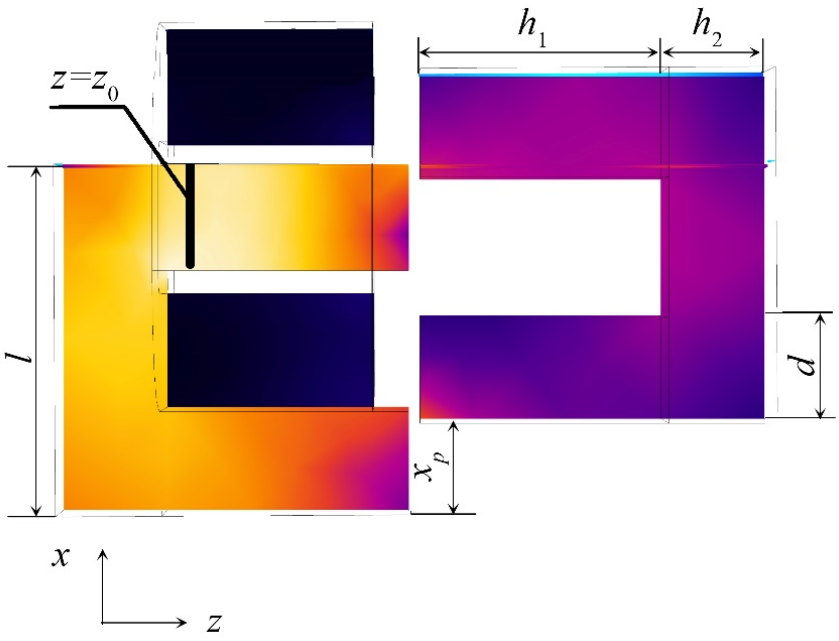

Figure 13 – Illustration to the choice of induction integration surface

First, we analyze the dependence of the factor of electromagnetic energy use k_f^* and the rotational force $F_{\Sigma x}$ on the width d of the teeth of U-shaped poles and on their mutual displacement x_p (Fig. 13). To do this, let's introduce the normalized offset parameter x^*:

$$x^* = \frac{x_p}{l}, \tag{17}$$

here l is the pole base length.

The dependences $F_{\Sigma x}(x^*)$ and $k_f^*(x^*)$ are obtained for the interval $x^* \in [0; 0.5)$ where the rotational force $F_{\Sigma x}$ is directed positively, and the pole tooth width d specifies as $2l/15$, $4l/15$, $5l/15$, $6l/15$, the pole base length l = 15 mm, the pole thickness w = 1 mm, the tooth height h_1 = 15 mm, the pole base width h_2 = 4.5 mm. The dependences $F_{\Sigma x}(x^*)$ and $k_f^*(x^*)$ at a constant current of the stator pole winding are shown in Fig. 14.

Fig. 14 (a) shows that a gradual increase in the pole tooth width d gives a positive effect on the initial stage – the interval Δx^* ,within which the force $F_{\Sigma x}$ is large than 70 % of its maximum value, increases as well as the force absolute value. However, when the pole tooth width d exceeds the value of one third of the pole base length l (d = 5 mm), a further increase in the parameter d, although leads to an increase in Δx^*, causes a significant decrease in the absolute values of the torque and the factor of energy use k_f^*. Therefore, when using rectangular poles, the effective control range of Δx^* is narrow and does not exceed 20% of the pole base length l. Further increase of the control range Δx^* is possible with a significant decrease in the factor of energy use k_f^*.

Fig. 14 shows a comparison of the rotational force $F_{\Sigma x}$ and the factor of energy use k_f^* depending on the coordinate x^* for a pole with a rectangular profile (curve 1), a trapezoidal pole with an extended profile (curve 2) and a trapezoidal pole with a

narrowed profile (curve 3).

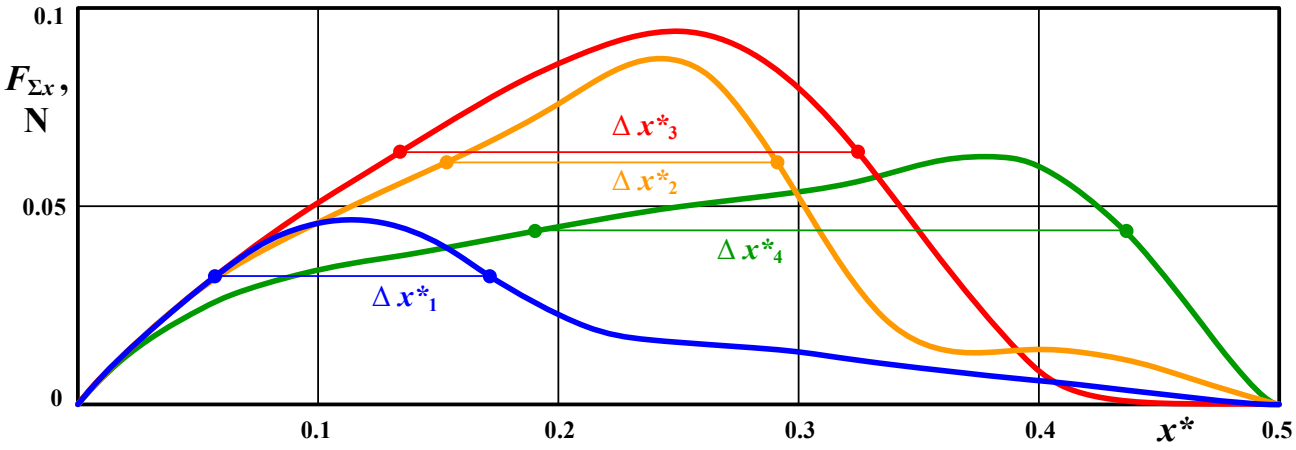

(a)

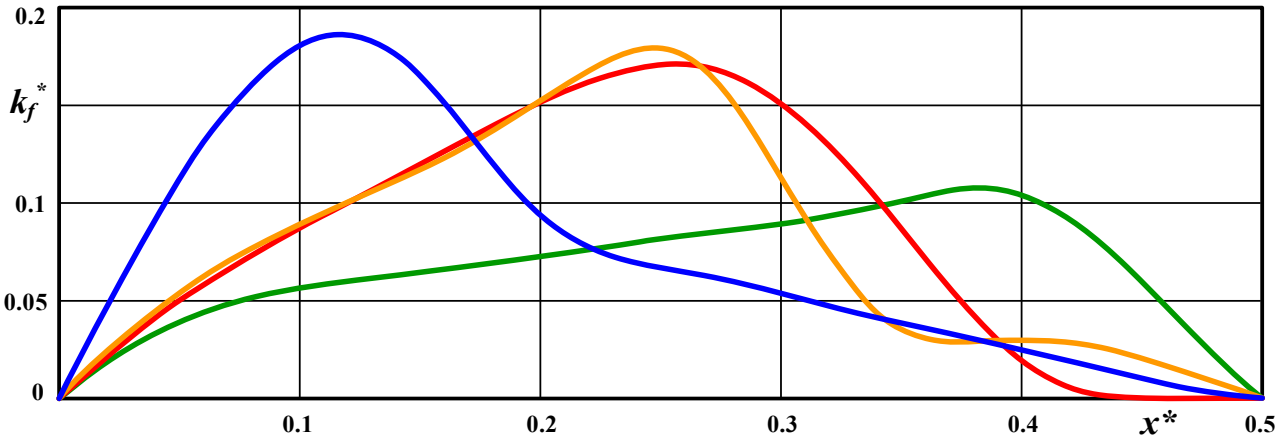

(b)

Figure 14 – The dependences for the pole with rectangular profile: (a) $F_{\Sigma x}(x^*)$, (b) $k_f^*(x^*)$

Analyzing Fig. 15, we can conclude that the use of the poles with a rectangular profile is more advisable for the proposed SRM design, as it provides the highest values of the rotational force and the factor of energy use. It should be noted that the decrease in the rotational force when using the trapezoidal pole with a narrowed profile is associated with an increase in the effective width of the air gap, whereas when using the trapezoidal pole with an extended profile it is associated with an increase in stray flux.

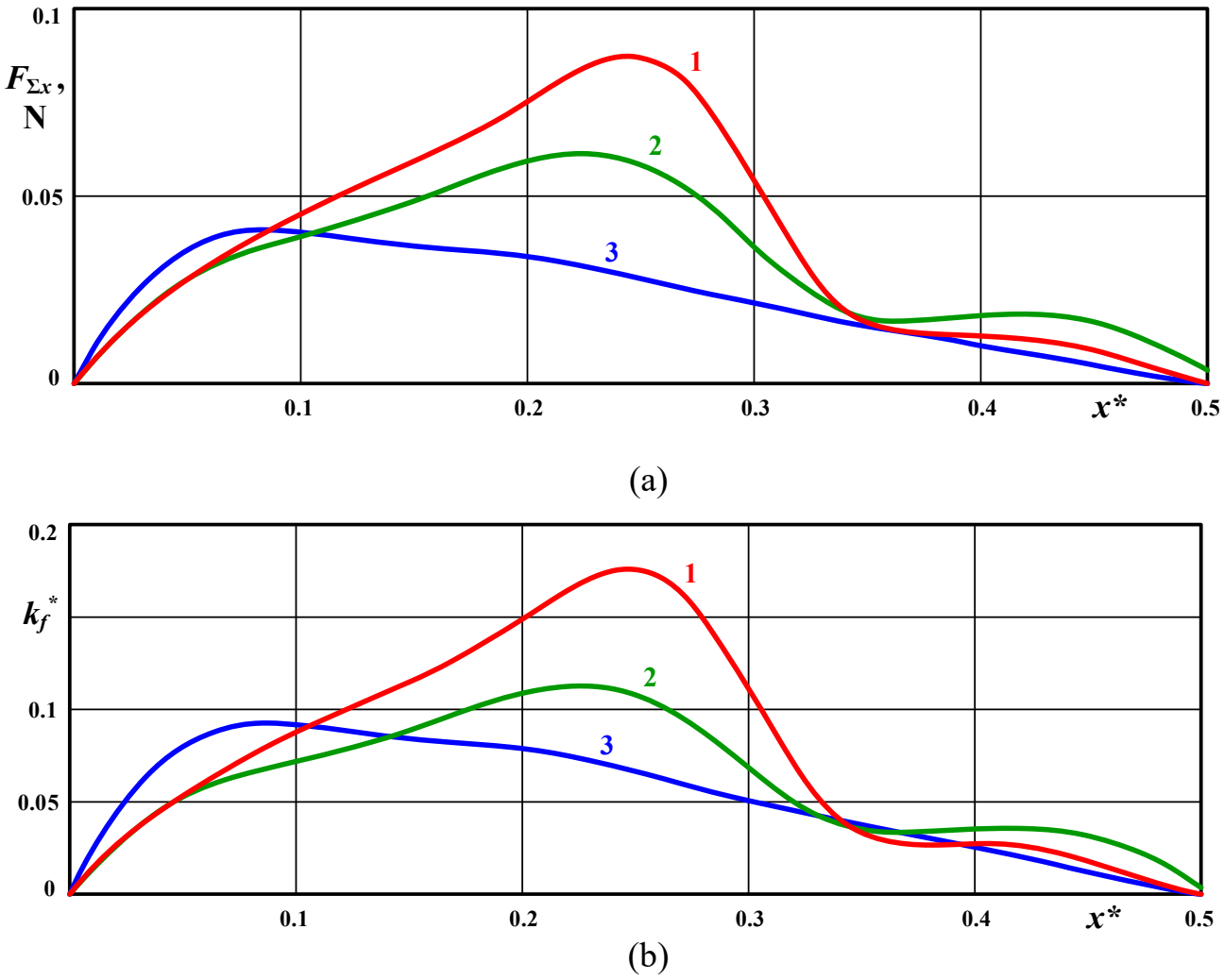

Figure 15 – A comparison of the dependencies for different pole shapes: (a) $F_{\Sigma x}(x^*)$, (b) $k_f^*(x^*)$

9.4. Minimizing the torque ripple of electric drive for switched reluctance motors

To increase the factor of energy use and to reduce the ripple of the torque, it is advisable to control the force F_Σ by changing the stator pole winding current according to a special law. Since the value of induction is proportional to the winding current, the force F_Σ is proportional to the square of the current (see (14)). Thus, to ensure the constant torque generated by the pole in a certain sector, it is necessary to form a special shape of the pole winding current. Because of that, the electric drive for the proposed SRM topology should meet the following requirements: the ability to regulate the output current shape, the ability to form steep edges of the current pulse, and the high efficiency.

Typically, SRMs are supplied with asymmetrical half-bridge converters [15]. Besides, shared topologies are used for more effective utilization of transistor switches [16, 17]. In order to improve converter efficiency, a soft switching control strategy and full-bridge topologies that allow synchronous rectifying [18] are used. In

the simplest case of SRM operation, the converter generates the constant current pulse in predefined stator pole winding based on the current chopping control that causes a significant torque pulsation. Some more advanced methods, for instance direct torque control [19] or use of torque sharing function [20] are able to reduce torque pulsation, however they involve the intersection of the currents of different poles of the stator that reduces SRM efficiency (Fig. 16).

The proposed control algorithm allows both to provide constant torque and to eliminate current intersection in SRM stator pole windings. The necessity of forming the sharp rising edge of winding current (Fig. 16, curve 3) makes it inappropriate to use the common asymmetrical half bridge converter because of its high operation frequency and thereby low efficiency. More attractive solution can be implemented in modular SRMs consisting of an even number of rotor and stator sections.

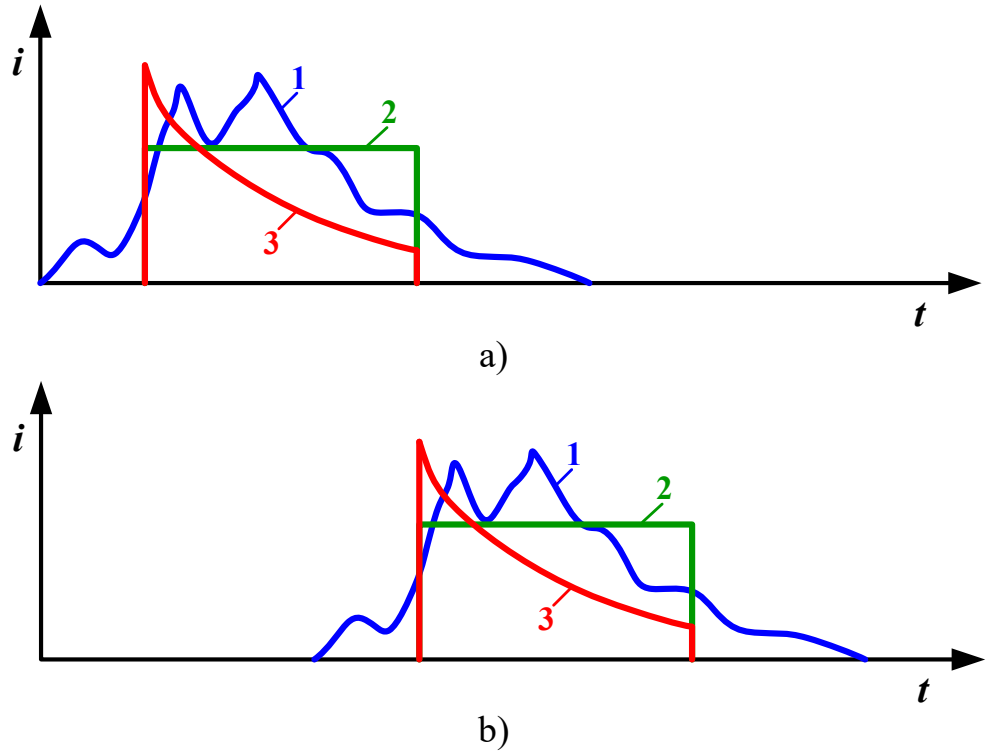

Figure 16 – Winding current shape in first pole (a) and second pole (b) of SRM: ***1 – direct torque control, 2 – current chopping control, 3 – proposed control.***

Let's consider a case of two-sectioned SRM. In such a motor, the total force F_Σ is a sum of the forces of the two sections, $F_{\Sigma 1}$ and $F_{\Sigma 2}$:

$$F_\Sigma = F_{\Sigma 1} + F_{\Sigma 2}. \tag{18}$$

As it was noted, the force F is proportional to second power of the winding current I, $F \sim I^2$. So, if we define the currents of the stator sections I_{SW1} and I_{SW2} as follows:

$$I_{SW1}(t) = I_{\Sigma}(t)\cos(\omega t); \tag{19}$$

$$I_{SW2}(t) = I_{\Sigma}(t)\sin(\omega t). \tag{20}$$

Then the total force F_{Σ} is proportional to the square of the total current:

$$F_{\Sigma} \sim I_{SW1}(t)^2 + I_{SW2}(t)^2 = I_{\Sigma}(t)^2, \tag{21}$$

and therefore it doesn't have pulsation as it's shown in Fig. 17.

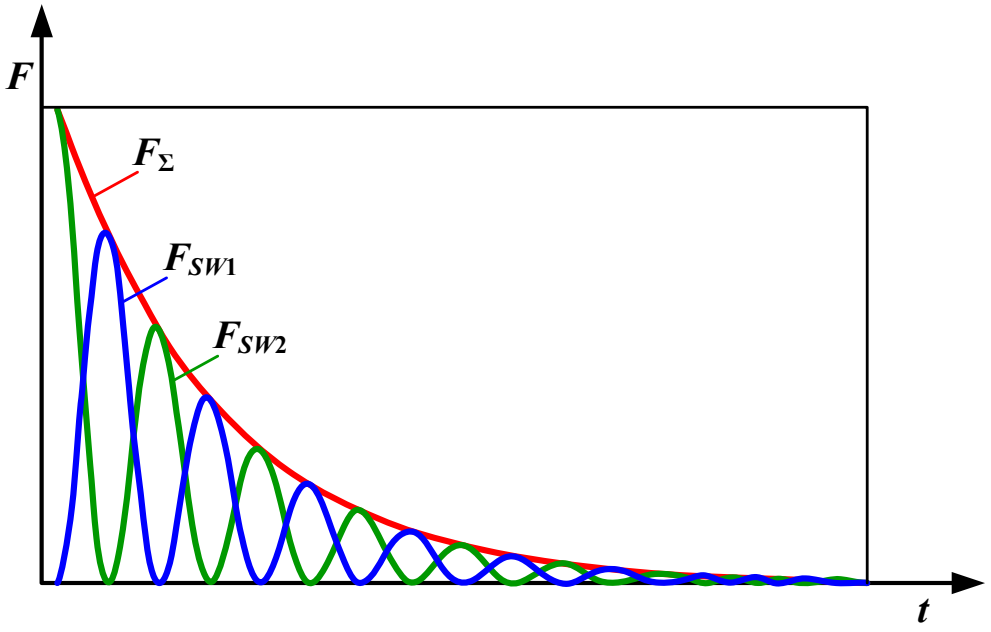

Figure 17 – The total force control in two-sectioned SRM

In conventional converter topologies, the regulation of the winding current amplitude in a wide range in accordance with a given shape of the total current $I_{\Sigma}(t)$ through harmonic currents as shown in formulas (22) and (23), requires more complex solutions, for example, two-stage conversion [21]. In single-stage converters, which are more efficient, it is advisable to regulate magnetic flux with additional stator winding. In this case, a total magnetic flux $\Phi_{SW(i)}$ of one SRM section is formed with two winding currents $I_{SW(i)1}$ and $I_{SW(i)2}$:

$$\Phi_{SW(i)}(t) \sim I_{SW(i)}(t) = I_{SW(i)1}(t) + I_{SW(i)2}(t). \tag{22}$$

If the current $I_{SW(i)1}$ is equal to $A\sin(\omega t)$ and the current $I_{SW(i)2}$ has the same amplitude A but is shifted the angle φ, $I_{SW(i)2} = A\sin(\omega t + \varphi)$, the section total flux $\Phi_{SW(i)}$ is calculated as follows:

$$\Phi_{SW(i)}(t) \sim 2A\sin(\omega t + \varphi/2)\cos(\varphi/2) = \\ = A^{*}\sin(\omega t + \varphi/2). \tag{23}$$

Therefore, it is possible to regulate the amplitude A^{*} in the range $[0; 2A]$ through

changing the angle φ.

The proposed way of the total force control has the following advantages:

- a possibility to form sharp rising edge of the current and subsequently of the total force;

- a high efficiency of motor drive due to transistor soft switching at current zero crossing time intervals.

As a basic topology providing the quasi-harmonic current shape given by formulas (19) and (20), a resonant bridge converter [22] shown in Fig. 18 can be used.

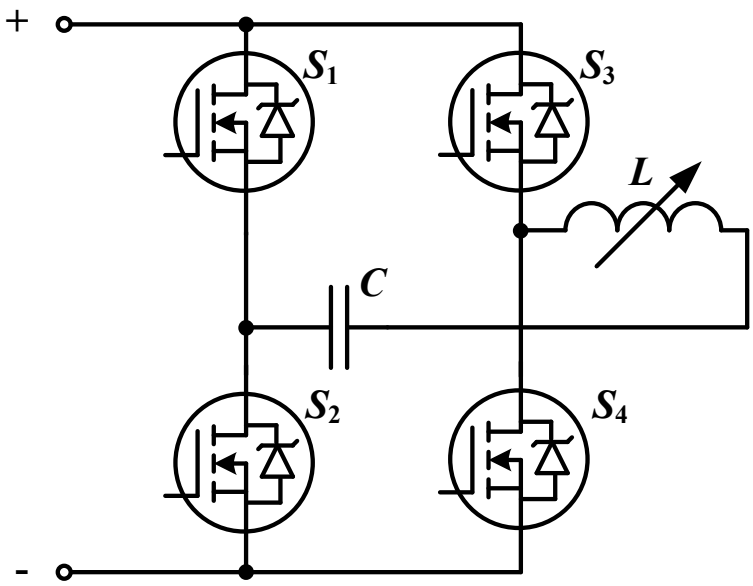

Figure 18 – Resonant bridge converter

The converter resonant circuit consists of a resonant capacitor C and a variable inductance of SRM stator pole winding L. The transistors S1-S4 are switched with the frequency

$$\omega = \frac{2}{\sqrt{LC}}, \tag{24}$$

at zero current.

The electric drive for one two-sectioned stator pole includes four identical resonant converters as shown in Fig. 19.

Such a modular drive structure additionally distributes the power among the converters [24].

As mentioned above, the stator poles operate one by one, therefore only one stator electric drive section can be used simultaneously. So, it may be connected to each stator pole via bidirectional switches S_{W11}- S_{W1n} and S_{W21}- S_{W2n} as shown in Fig. 20.

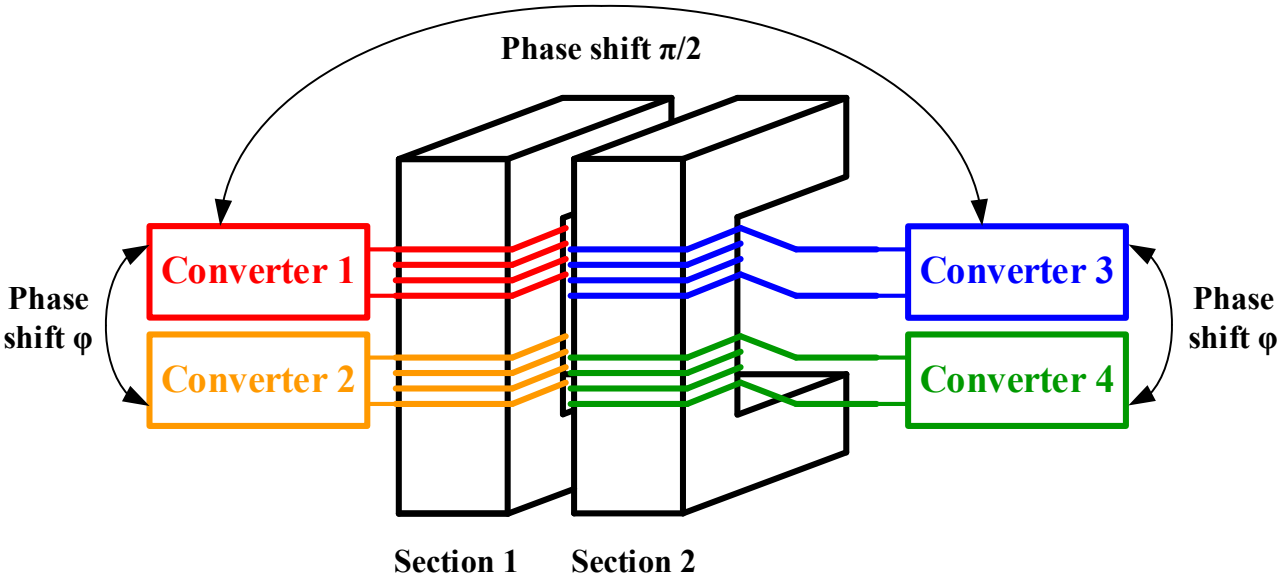

Figure 19 – Electric drive for one two-sectioned stator pole

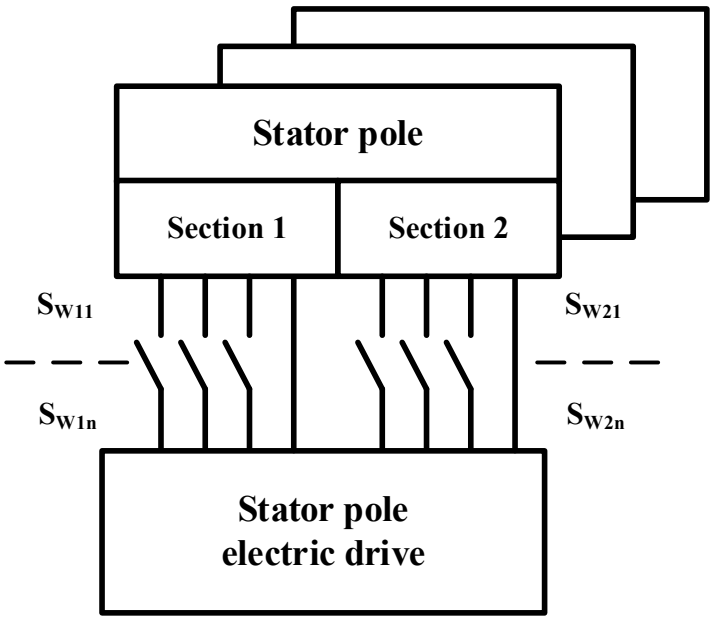

Figure 20 – Proposed SRM electric drive structure

SRM electric drive model is designed in MATLAB Simulink®. One converter model is shown in Fig. 21 (a) and a full SRM drive model is shown in Fig. 21 (b).

The following values of the parameters of the resonant elements are used in the simulation: variable winding inductance $L = 10^{-4}...10^{-3}$ H, capacitance of the resonant capacitor $C = 10^{-4}$ F.

The diagrams of the section winding currents and the section forces over time are shown in Fig. 22 (a) and (b) respectively.

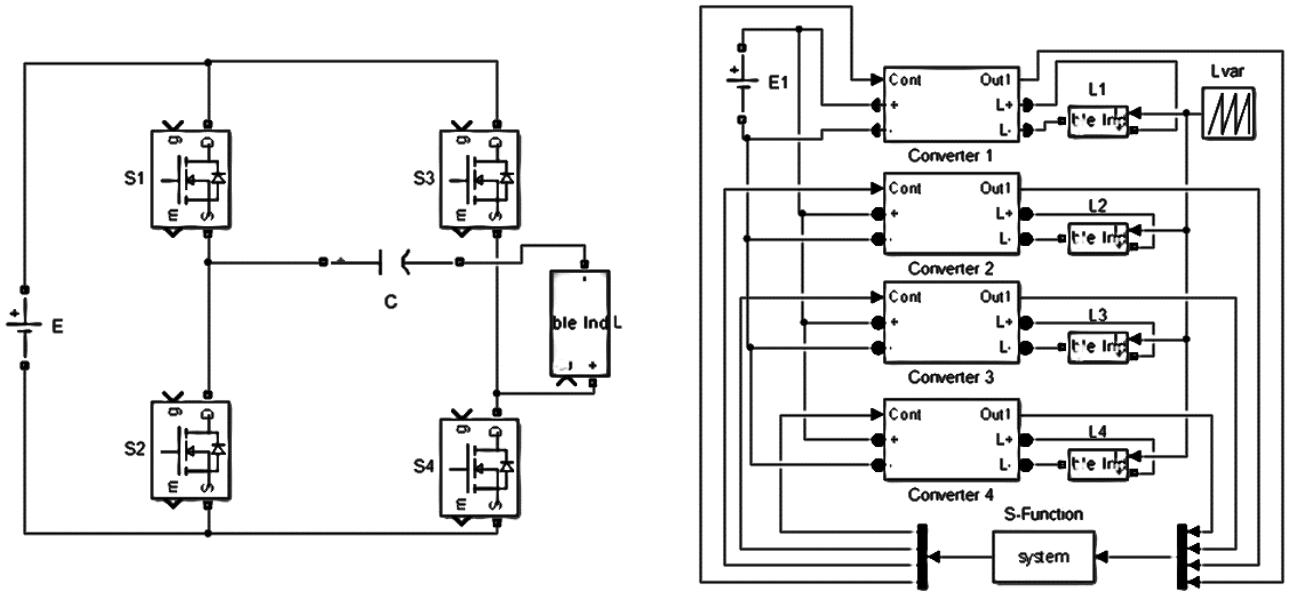

(a) (b)

Figure 21 – SRM model: (a) one converter model, (b full SRM drive model

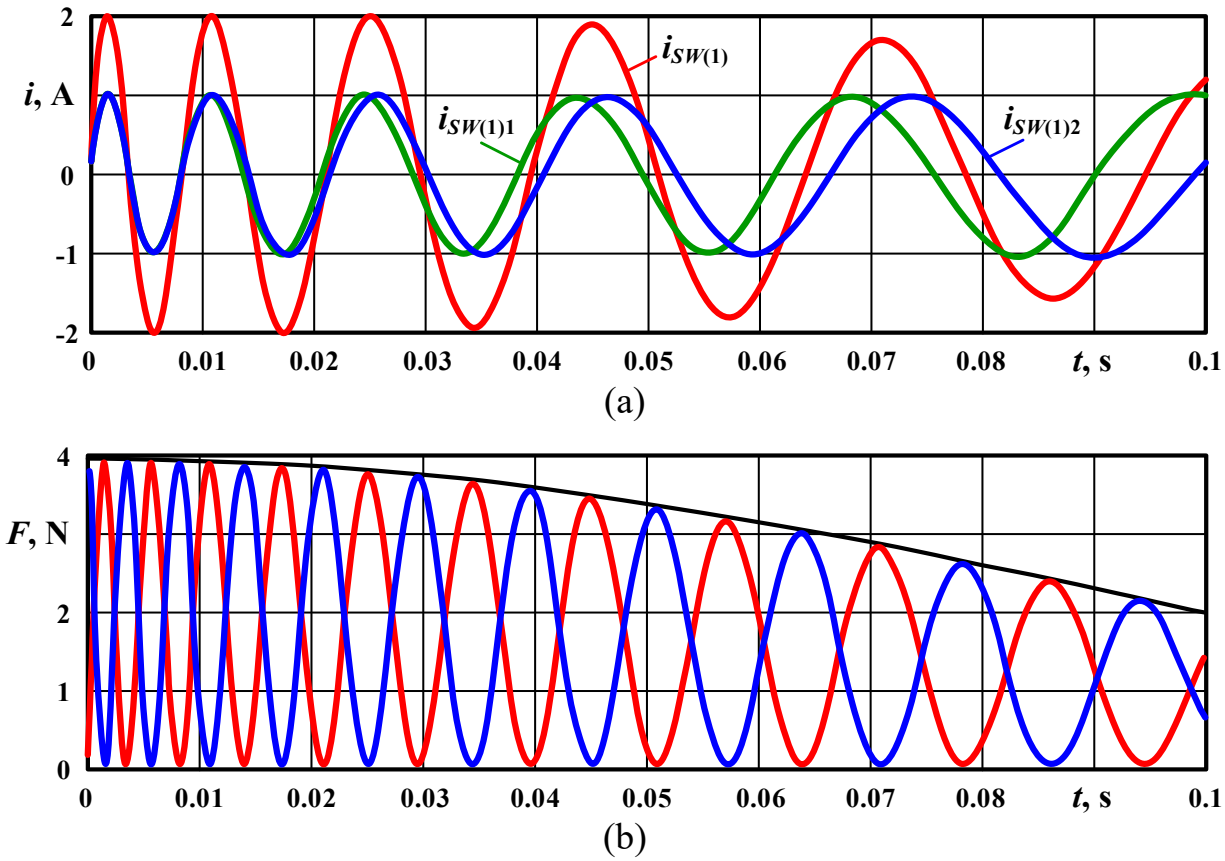

(a)

(b)

Figure 22 – The diagrams over time: (a) section currents, (b) SRM forces

As we can see in Fig. 22 (a), the phase shift control of two section currents $I_{SW(1)1}$ and $I_{SW(1)2}$ of the stator pole makes it possible to regulate the amplitude of the equivalent current $I_{SW(1)}$ that allows to obtain the total force F_Σ without pulsation as

considered in the theory.

Conclusions

1. Although the brushless synchronous DC motors with permanent magnets are a kind of standard in electric cars today, the steady development of technologies and design ideas as well as the changes in the market conditions for motor components of electric vehicles lead to the fact of rising the interest to other decisions. So that, simple and cheap switched reluctance motors are considered now as promising alternative, that makes the studies directed to enhancing their characteristics highly relevant.

2. The disadvantages of classical switched reluctance motors, such as low specific torque and its significant ripple, caused by their design features and operation principles can be eliminated by forming a special current shape in the stator windings and by improving the motor topology through optimizing the shape of the poles and their ratio.

3. A new represented topology of SRM has U-shaped stator and rotor poles. It characterized by reducing the magnetic material and the total weight of the motor. The modular structure of the stator and rotor poles makes it possible to produce them separately by cheaper technology comparing to a classical SRM topology. To provide the higher density of the poles and so prevent the reduction of the specific torque, it is proposed to use paired windings for the stator poles.

4. It was defined that to ensure efficient motor operation the condition $l_{leak} >> l_g$ (where l_{leak} and l_g are the air gap between the stator pole teeth and the stator and rotor poles' gap respectively) should be kept during the entire operating time. Another important condition is the tendency of the braking force F_{br} to zero, which requires the working rotor pole to be as close as possible to corresponding stator pole when activating it during rotor rotation.

5. The SRM topology with U-shaped poles placed in accordance with $(n+1)/n$ ratio, where numerator is the stator pole number and the denominator is the rotor pole number, provides a higher density of the rotor poles' location relative to the stator ones, which makes it possible to obtain a higher accelerating force, so, this topology is considered as more preferable in practice.

6. In order to verify the theoretical positions, a motor with U-shaped poles located by $(n+1)/n$ topology at $n = 7$ and with the simultaneous control of three poles was developed and calculated. As a result, the developed motor with the dimensions $l = 313$ mm, $D = 520$ mm provides a torque 1150 N/m and has a maximum speed 9375 rpm. The losses on the magnetic circuit magnetization reversal at the maximum operating frequency amounted to 8%.

7. The analysis of the simulation results showed that the use of the poles with a rectangular profile is more advisable for the proposed U-shaped pole SRM design, as it provides the highest values of the rotational force and the factor of energy use.

8. The electric drive for the proposed SRM topology with U-shaped poles should meet the following requirements: the ability to regulate the output current shape, the ability to form steep edges of the current pulse, and the high efficiency. A

resonant bridge converter is chosen as an effective basic circuit providing the needed quasi-harmonic current shape of the stator pole winding.

9. The use of modular SRM topology consisting of an even number of rotor and stator sections makes it possible to implement the effective phase shift control method providing the formation of sharp rising edge of the current and subsequently of the motor total force, a stability of the motor total force without pulsation, and a high efficiency of motor drive due to transistor soft switching at current zero crossing time intervals.